doi:10.1093/brain/awt327 Brain 2014: 137; 420–432 | 420

BRAIN
A JOURNAL OF NEUROLOGY

Neuronal merlin influences ERBB2 receptor expression on Schwann cells through neuregulin 1 type III signalling

Alexander Schulz,[1,*] Anna Kyselyova,[2,*] Stephan L. Baader,[3] Marie Juliane Jung,[1] Ansgar Zoch,[1] Victor-Felix Mautner,[4] Christian Hagel[2,†] and Helen Morrison[1,†]

1 Leibniz Institute for Age Research, Fritz Lipmann Institute, 07745 Jena, Germany
2 Institute of Neuropathology, University Medical Centre Hamburg-Eppendorf, 20246 Hamburg, Germany
3 Institute of Anatomy, Anatomy and Cell Biology, University of Bonn, 53115 Bonn, Germany
4 Department of Neurology, University Medical Centre Hamburg-Eppendorf, 20246 Hamburg, Germany

*These authors contributed equally to this work.
†These authors contributed equally to this work.

Correspondence to: Prof. Dr. Christian Hagel,
Institute of Neuropathology,
University Medical Centre Hamburg-Eppendorf,
Martinistrasse 52,
D-20246 Hamburg,
Germany
E-mail: hagel@uke.uni-hamburg.de

Correspondence may also be addressed to: Dr. Helen Morrison, Leibniz Institute for Age Research, Fritz Lipmann Institute, Beutenbergstrasse 11, D-07745 Jena, Germany, E-mail: helen@fli-leibniz.de

Axonal surface proteins encompass a group of heterogeneous molecules, which exert a variety of different functions in the highly interdependent relationship between axons and Schwann cells. We recently revealed that the tumour suppressor protein merlin, mutated in the hereditary tumour syndrome neurofibromatosis type 2, impacts significantly on axon structure maintenance in the peripheral nervous system. We now report on a role of neuronal merlin in the regulation of the axonal surface protein neuregulin 1 important for modulating Schwann cell differentiation and myelination. Specifically, neuregulin 1 type III expression is reduced in sciatic nerve tissue of neuron-specific knockout animals as well as in biopsies from seven patients with neurofibromatosis type 2. *In vitro* experiments performed on both the P19 neuronal cell line and primary dorsal root ganglion cells demonstrate the influence of merlin on neuregulin 1 type III expression. Moreover, expression of ERBB2, a Schwann cell receptor for neuregulin 1 ligands is increased in nerve tissue of both neuron-specific merlin knockout animals and patients with neurofibromatosis type 2, demonstrating for the first time that axonal merlin indirectly regulates Schwann cell behaviour. Collectively, we have identified that neuronally expressed merlin can influence Schwann cell activity in a cell-extrinsic manner.

Keywords: axon; merlin; myelination; neuregulin 1; neurofibromatosis type 2; polyneuropathy; Schwann cell
Abbreviation: NF2 = neurofibromatosis type 2

Received May 7, 2013. Revised September 9, 2013. Accepted September 30, 2013. Advance Access publication December 5, 2013

Introduction

The development and lifelong integrity of myelinated peripheral nerves rely on the co-ordinated, reciprocal communication between axons and Schwann cells. In addition to intrinsic factors that modify the properties of myelin-producing Schwann cells, several extrinsic regulators of myelination derived from axons have been described. Axons provide signalling cues to Schwann cells influencing proliferation, differentiation and survival of Schwann cells during development as well as in the adult ensuring the lifelong maintenance and preservation of a functional nerve (Michailov *et al.*, 2004; Taveggia *et al.*, 2005).

One of the best characterized signalling cascades between axons and Schwann cells is the neuregulin 1 (NRG1)–ERBB2/3 pathway, interference of which results in Schwann cell defects leading to degeneration of motor and sensory neurons (Corfas *et al.*, 2004). The NRG1 growth factor-like family exists in various isoforms due to alternative splicing (Kerber *et al.*, 2003). NRG1 type I and II are shed by axons, acting as paracrine signals, whereas type III is cleaved but remains tethered to the axon surface, acting as a juxtacrine signal (Nave and Salzer, 2006). All of these axon-derived NRG1 family members influence multiple and distinct phases of Schwann cell development by binding and signalling through the ERBB2/3 receptor tyrosine kinases on Schwann cells (Morrissey *et al.*, 1995; Vartanian *et al.*, 1997; Rahmatullah *et al.*, 1998).

NRG1 type III is a key instructive signal for Schwann cell myelination through phosphoinositide 3-kinase (PI-3K)/Akt activity downstream of the ERBB2/3 receptor (Taveggia *et al.*, 2005). Moreover, the expression levels of NRG1 type III are thought to determine the myelination fate of axons (Quintes *et al.*, 2010). Large calibre axons will only be myelinated when expressing high levels of NRG1 type III compared with the low levels found on small calibre fibres that are organized in Remak bundles. Forced expression of NRG1 type III in normally non-myelinated fibres results in ectopic myelination (Taveggia *et al.*, 2005), whereas reductions in NRG1 type III result in significant hypomyelination. These findings indicate that Schwann cells can sense and then decide to myelinate dependent on the amount of NRG1 type III presented to them.

Neurofibromatosis type 2 (NF2) is an autosomal dominant inherited syndrome characterized by mutations in the gene coding for the tumour suppressor merlin located on chromosome 22q 11.2. Patients with NF2 typically develop tumours of the PNS and CNS (Baser *et al.*, 2003). A diagnostic hallmark of NF2 is bilateral schwannomas of the vestibular nerve. Some patients with NF2 additionally suffer from severe generalized peripheral polyneuropathy, which does not correlate with tumour burden (Hagel *et al.*, 2002). As a possible cause for a non-tumorigenic aetiology of the polyneuropathy, recent studies have revealed that merlin expressed in neurons is capable of regulating different steps of neuromorphogenesis through small GTPase activity control (Schulz *et al.*, 2010). Furthermore, merlin in PNS neurons has been shown to impact on axon structure maintenance through neurofilament phosphorylation in an axon-intrinsic manner (Schulz *et al.*, 2013). Specifically, the loss of one merlin splice variant, namely merlin isoform 2, results in both irregular-shaped PNS axons and altered ultrastructural neurofilament composition, leading to neuropathic symptoms in a merlin-mutant mouse model. These findings indicate that reduced gene dosage of merlin in neurons contributes to the pathogenesis of NF2-related polyneuropathy even in the absence of nerve-damaging schwannomas.

Axonal pathologies have been shown to precede demyelination or cause secondary Schwann cell effects (Vavlitou *et al.*, 2010). We therefore hypothesized that the reduction of neuronal merlin resulting in axonal atrophy may also affect the crosstalk between axons and Schwann cells. Using merlin-mutant mouse models, we therefore investigated whether any Schwann cell changes could be detected *in vivo*. Moreover, because it has been proposed that, dependent on the axonal dimension, neurons regulate NRG1 type III expression (Michailov *et al.*, 2004), we further examined if the expression of this axonal membrane-associated growth factor is altered, possibly leading to aberrant NRG1–ERBB2/3 signalling between axons and Schwann cells. Such a deregulation of axonally-derived Schwann cell fate determinants could mechanistically play a role in the development of neuropathies. Furthermore, Schwann cell detachment from axons may constitute an important early event for Schwann cell-derived tumours observed in NF2 (Miller *et al.*, 2003).

Materials and methods

Experimental animals

All mice used in this study were handled in strict adherence to local governmental and institutional animal care regulations. Animals had free access to food and water and were housed under constant temperature and humidity conditions on a 12/12-h light/dark cycle. The following transgenic mouse strains were used for the study: *Nf2* iso1 knockout and *Nf2* iso2 knockout mice, generated by Dr. Michiko Niwa-Kawakita and Dr. Marco Giovannini, were purchased from RIKEN BioResource Centre. Nf2flox animals (RIKEN BioResource Centre) were used to obtain conditional, Schwann cell-specific merlin knockout by crossing with the P0-Cre line (The Jackson Laboratory, stock 017928). To achieve neuron-specific loss of merlin *in vivo*, we mated Nf2flox animals with a mouse strain that expresses Cre recombinase under the neurofilament heavy class promoter (Nefh-Cre) (The Jackson Laboratory, stock 009102). Offspring of Nf2flox and Stra8-Cre animals were used to produce $Nf2^{\Delta/fl}$ mice. The Stra8-Cre mouse line deletes the targeted gene—in this case the *Nf2* gene—in germ cells of males, thus resulting in the same gene disruption in all progeny.

All animals were on a C57BL/6 background. The day of birth, on average the 19th day of pregnancy, was defined as post-natal Day 0. Tissue was taken from 8-week-old, adult mice unless stated otherwise. Genotyping was performed according to the recommendations of the manufacturer or depositor, respectively.

Sural nerve biopsies from patients with neurofibromatosis type 2

Nine sural nerve biopsies from seven patients with NF2 were investigated. The patients that met the NIH criteria for NF2 (Gutmann *et al.*, 1997) and were diagnosed according to the Manchester criteria (Baser *et al.*, 2003), were included in this study. Informed consent was obtained from all patients. Clinical characteristics of the patients, including

age at operation, gender and severity of disease, were obtained by review of the medical records. Neurological examination was performed in all patients and electrophysiological examination was conducted in patients with suspected polyneuropathy. Metabolic, inflammatory, toxic or genetic reasons other than NF2 were excluded as a reason for polyneuropathy by medical history and examination of blood and CSF (Hagel *et al.*, 2002). The cohort comprised five male and two female patients; the mean age of patients at operation was 44 ± 11.6 years.

As controls, 12 sural nerve specimens with normal histomorphology were selected (mean age 55 ± 11.96 years, male:female = 9:3). Further, to study possible changes in NRG1 expression in other pathological conditions, 10 samples with chronic inflammatory demyelinating polyneuropathy and nine samples with non-inflammatory chronic axonopathy were investigated (mean age 66 ± 12.87 years for patients with chronic inflammatory demyelinating polyneuropathy, male:female = 3:7; 58 ± 14.45 years for patients with axonopathy, male:female = 8:1).

Histopathology and immunohistochemistry of sural nerve biopsies

All sural nerve specimens were primarily diagnosed in the Institute of Neuropathology, University Medical Centre Hamburg-Eppendorf, by two neuropathologists. For routine diagnostics, formalin-fixed and paraffin-embedded material was stained with haematoxylin and eosin, periodic acid-Schiff, Elastica van Gieson, Masson-Goldner, Turnbull, Congo red, thioflavin-S and Bodian's stains. Semi-thin sections of the NF2 sural nerves were stained with toluidine blue. In addition, the samples were labelled with antibodies against neurofilament, S-100 protein, leukocyte common antigen, CD79a, CD45R0, HLA-DR/DP/DQ, CD68, CD4, CD8, CD20, Ki-67 and epithelial membrane antigen.

For the present investigation, the NF2 samples, controls, chronic inflammatory demyelinating polyneuropathy and axonopathy cases were double-labelled immunohistochemically with antibodies against neurofilament and myelin protein zero, NRG1 and myelin protein zero or single labelled with antibodies against ERBB2. Specimens of breast cancer metastases previously found to express ERBB2 served as a positive control for labelling with ERBB2 antibodies (Maguire and Greene, 1990). As a second positive control, sural nerve biopsies with severe vasculitic changes were selected (Massa *et al.*, 2006). The sciatic nerves from four mice were single-labelled with antibodies against neurofilament, NRG1 and ERBB2.

All slides were coated with poly-L-lysine (10%, Sigma Aldrich, #P8920) for improved adhesion of the sections. Staining of human tissue took place in an automated stainer (Ventana Medical Systems) using a standard antigen retrieval protocol (CC1). The specimens were double-labelled with antibodies against neurofilament (1:800, DakoCytomation) and myelin protein zero (1:300, Bioss Antibodies) or NRG1 (1:200, Acris Antibodies) and myelin protein zero and single-labelled against ERBB2 (1:100, DakoCytomation). Bound neurofilament-, NRG1- and ERBB2-antibodies were detected by the peroxidase method using diaminobenzidine as chromogen (Ventana Medical Systems), whereas myelin protein zero was demonstrated using the alkaline phosphatase method and fast red as chromogen (Ventana Medical Systems). All slides were counterstained with alum-haematoxylin.

Immunohistochemistry of mouse nerve specimens was performed in a similar way for neurofilament, whereas NRG1 and ERBB2 labelling was conducted using Shandon cover plate immunostaining chambers (Thermo Scientific). Tissue was processed and sectioned similarly to human samples. After rehydration and blocking of endogenous peroxidase with 0.3% H_2O_2 for 15 min, the slides were boiled in a microwave oven for 60 min at 640 W in 10% citrate buffer (pH 6.0) for antigen retrieval. NRG1 (1:100) and ERBB2 antibodies (1:50) were applied overnight at 5°C. Ventana Medical Systems' kit (see above) was applied as secondary antibody for 90 min at 5°C. Bound secondary antibodies were visualized with diaminobenzidine. Slides were counterstained with Mayer's haemalum (1:1, Merck) for 30 s.

Evaluation of stainings

Two out of nine sural nerve biopsies of patients with NF2 were devoid of axons and so were excluded from the present study. Double-labelled sections were evaluated quantitatively by calculating the percentage of nerve fibres positive for NRG1 and myelin protein zero against all myelin protein zero-positive fibres in the same fascicle. To ensure that all myelin protein zero-positive myelin sheaths contained an axon, NRG1/myelin protein zero labelling was compared with samples double-labelled with myelin protein zero and neurofilament antibodies. ERBB2-labelled sections were assessed in a similar way by calculating the percentage of ERBB2-positive fibres in relation to all fibres in the same fascicle analysed for neurofilament and NRG1 expression.

Single-stained mouse nerve sections were evaluated quantitatively in three fascicles. Each fascicle was photographed and the images were combined using AxioVision Software V4.6.2. Myelinated nerve fibres were marked with red or green dots in the images to denote NRG-positive (strong or moderate labelling) or NRG-negative (no or slight labelling), respectively. The dots were counted with AxioVision and related to the total area of the fascicle to obtain the fibre density. Fibre densities of NRG-positive and NRG-negative fibres were summed to attain the total fibre density. Finally, the percentages of NRG-positive fibres were calculated by dividing the density of NRG-positive fibres by the density of all fibres and multiplying by 100. ERBB2-labelled sections were analysed as described above.

Immunoblotting

Immunoblotting was performed as described by Morrison *et al.* (2001). The following primary antibodies were used: anti-merlin (1:500, Santa Cruz Biotechnology, clone A-19), anti-actin (1:2000, Santa Cruz Biotechnology, clone I-19), anti-Nrg1 (1:250, Santa Cruz Biotechnology, clone C-20), anti-Notch1 (1:1000, Santa Cruz Biotechnology, clone C-20), anti-Akt (1:500, Cell Signaling), anti-phospho-Akt (S473, 1:500, Cell Signaling), anti-Erk (1:500, Cell Signaling), anti-phospho-Erk (T202/Y204, 1:500, Cell Signaling), anti-Nrg1 (1:250, clone C-20), anti-ErbB2 (1:500, Cell Signaling), and anti-Tau (1:500, Cell Signaling). Western blot results were quantified using Gel analysis software by ImageJ. Density values were normalized to actin and appropriate controls of transfection or wild-type tissue, respectively. In case of phospho-specific detection of proteins, their acquired densities were referred to signals derived from related pan-antibodies (e.g. phospho-Akt to Akt signals).

Reverse-transcription polymerase chain reaction analysis

Total RNA was isolated from cultured and transfected P19 cells using RNA Mini Kit (Qiagen) according to the manufacturer's instructions. Complementary DNA was reverse transcribed with random hexamers by reverse transcriptase SuperScript® III (Invitrogen). PCR amplification was performed with Taq DNA polymerase (Fermentas) for 35 cycles at 94°C for 1 min, 60°C for 1 min, and 72°C for 1 min. Oligonucleotides

for amplifying the EGF domain of Nrg1 were 5′-GCA TGT CTG AGC GCA AAG AAG-3′ (forward) and 5′-CGT TAC TTG CAC AAG TAT C-3′ (reverse) as previously described (Zhang *et al*., 2011).

P19 cell culture

P19 cells were purchased from ATCC (CRL-1825) and maintained in Dulbecco's modified Eagle's medium supplemented with 10% foetal calf serum. For induction of a neuronal phenotype, aggregates were generated on bacterial-grade dishes and treated with 5×10^{-7} M all-trans retinoic acid (Sigma Aldrich) for 4 days. Subsequently, cells were replated on dishes of cell culture grade in the absence of retinoic acid.

Site-directed mutagenesis

QuikChange® Site-Directed Mutagenesis Kit (Stratagene) was used according to the manufacturer's instructions to generate C-terminal merlin point mutation carrying mutants Q324L, K413E and L535P.

Dorsal root ganglion culture

Preparation of dorsal root ganglion cells from 4- to 6-day-old mice (P4–P6) was performed as described in Malin *et al*. (2007). Arabinofuranosyl cytidine (working concentration of 10 μM, Sigma Aldrich) was used to ensure glia-free conditions.

Transfection procedure

P19 and primary dorsal root ganglion cells were transfected 3–4 days after plating using Lipofectamine® 2000 (Invitrogen) according to the manufacturer's protocol. Transfection efficiency averaged between 40 and 50%.

Immunocytochemistry

Primary dorsal root ganglion cells were grown on coverslips and fixed with 4% paraformaldehyde in PBS for 20 min. After washing in PBS, cells were permeabilized with 0.3% Triton™ X-100 for 1 min and incubated for 2 h in 1% bovine serum albumin. Subsequently, cells were incubated with the primary antibodies at room temperature for 1 h. The following antibodies were used: anti-phospho neurofilament (1:200, Hiss Diagnostics) and anti-Nrg1 (1:40, Santa Cruz Biotechnology, clone C-20, sc-348). Following extensive rinsing in PBS, cells were incubated with secondary antibodies linked to Alexa Fluor® 488 (1:500, anti-rabbit) or Alexa Fluor® 546 (1:500, anti-mouse) for 1 h. Cells were then washed in PBS and counterstained with Hoechst 34580 (1:1000 in PBS) for 5 min. Finally, cells were mounted on cover plates with a Mowiol®-based mounting medium.

Microscopy and image acquisition

Fluorescent images of dissociated neurons were obtained with a Zeiss Axio Imager ApoTome microscope (Zeiss). All digital processing of the photomicrographs was performed using Adobe Photoshop 6.0. For all images, only linear adjustments of the brightness and contrast were performed.

Immunofluorescence of murine sciatic nerve cross-sections

Paraffin–embedded sections were rehydrated, boiled in 10 mM sodium citrate buffer (pH 9) for 30 min in a microwave and subsequently treated with 0.5% Triton™ X-100 for 10 min. Sections were incubated in 0.2% gelatine and 2% goat serum diluted in PBS for at least 2 h. The sections were submersed in the primary antibody solution overnight at 4°C. The following primary antibodies were used: anti-phospho-Akt (S473, 1:200, Cell Signaling), anti-phospho-Erk (1:200, Santa Cruz Biotechnology, clone E4, sc-7383), anti-S100 (1:200, Santa Cruz Biotechnology, clone N-15, sc-7852) and anti-phospho neurofilament (1:500, Hiss Diagnostics). After vigorous washing, sections were incubated with secondary antibody solution (Alexa Fluor® 488- and Alexa Fluor® 546-conjugated goat anti-mouse and -rabbit antibodies, 1:500 in PBS, Invitrogen) at room temperature for 2 h. Finally specimens were washed in PBS, counterstained using Hoechst 34580 (1 μg/ml PBS, 5 min), dehydrated and embedded.

Analysis of myelination in merlin knockout mice

Analysis of axon calibre and myelination was conducted on semi-thin and ultra-thin sections of the sciatic nerve removed from transcardially perfused mice. Mice were perfused with a solution containing 3% paraformaldehyde and 3% glutaraldehyde in 0.1 M phosphate buffer (pH 7.4). Sections were postfixed for 1 h and kept in fixative including 3% sucrose. Sections were obtained from the mid-part of the sciatic nerve reaching from the gluteal to the popliteal regions. Sectioning and staining were performed as described. Images of toluidine blue-stained semi-thin sections were taken using an Axioskop 2 MOT (Carl Zeiss) equipped with a ×100 immersion oil objective and an Olympus XC50 digital camera (Olympus). Standardized settings for camera sensitivity, resolution (2576 × 1932 pixels) and brightness of illumination were used for all micrographs. Ultra-thin sections were analysed with an electron microscope (EM910, Carl Zeiss) equipped with an integrated TRS 1K digital camera (Carl Zeiss). Image analysis was conducted with ImageJ version 1.43u. RGB colour images obtained from semi-thin sections were split into single channels and the green channel was chosen for measurements. The image was contrasted using the auto function. Using the freehand selection tool, the axon and the myelin were grossly circumscribed and the area adapted using the ABSnake plugin (the gradient threshold varied between 20 and 30, 10 to 20 iterations were used per image). Low contrasted myelin sheaths were surrounded manually. Based on the measured areas, the thicknesses of the axons and myelin sheaths were calculated.

Statistical evaluation

All statistics were performed using SPSS for Windows version 20. Significance levels were calculated using Student *t*-test or one-way ANOVA. Multiple correlations between the variables were computed using the Kendall tau-b test.

Results

Neuregulin 1 expression in merlin knockout animals

To investigate whether the expression of axonal surface proteins is dependent on merlin levels in neurons, we first analysed sciatic nerve lysates derived from adult merlin isoform-specific knockout mice. We focused on the neuregulin family of proteins as well as NOTCH1 as obvious axonal membrane molecules. In particular,

NRG1 type III represented a reasonable candidate to study because it is thought to act as a biochemical sensor of axon calibre (Michailov *et al.*, 2004). The NRG1 type III full-length protein is processed to its biologically active form (75 kDa) by proteolytic cleavage (Velanac *et al.*, 2012). Developmental analysis of NRG1 isoforms revealed a clear correlation between the active form of NRG1 type III and the onset of myelin basic protein expression, a marker for myelination, in sciatic nerves (Supplementary Fig. 1). Except for early post-natal time points, NRG1 type III showed the highest expression levels when compared with NRG1 types I and II (Supplementary Fig. 1), which is in line with previous reports (Liu *et al.*, 2011).

It has been previously suggested that—dependent on their axonal diameter—neurons themselves can regulate NRG1 type III expression (Michailov *et al.*, 2004). We therefore expected that only merlin isoform 2 (merlin-iso2) knockout mice, associated with axon-intrinsic pathology (Schulz *et al.*, 2013), would carry altered NRG1 type III. Surprisingly, however, we found that nerve lysates of both merlin isoform 1 (merlin-iso1)-deficient animals and merlin-iso2-deficient animals showed decreased levels of NRG1 type III (Fig. 1A), indicating that axonal integrity is uncoupled from NRG1 type III regulation. The PI-3K/Akt signalling pathway downstream of ERBB2/3 receptor has been shown to be a key signalling event for myelination of Schwann cells (Taveggia *et al.*, 2005). As expected, lysates with reduced NRG1 type III also carried reduced phosphorylation levels of Akt (p-Akt; Fig. 1A). Another prominent axonal surface protein, Notch1, also appeared to be decreased in sciatic nerve lysates following the loss of either merlin isoform 1 or 2 (Fig. 1B).

Although NRG1 type III exclusively appears on axonal surfaces as a juxtacrine signalling molecule, both Schwann cells and neurons express NOTCH1 (Yoon and Gaiano, 2005; El Bejjani and Hammarlund, 2012). To identify the cellular compartment responsible for the merlin-dependent deregulation of the respective axonal surface proteins, we used an established mouse model mimicking NF2 disease where the Schwann cell-specific promoter myelin protein zero (P0) conditionally deletes merlin in Schwann cells (P0-Cre;Nf2flox). The loss of merlin in Schwann cells (P0-Cre;Nf2$^{fl/fl}$) had no effect on NRG1 type III levels (Fig. 1C), whereas NOTCH1 expression was markedly reduced (Fig. 1D) compared to wild-type littermates (P0-Cre;Nf2$^{+/+}$). These findings suggest that axonal NRG1 is not influenced by the loss of merlin in Schwann cells. On the other hand, diminished expression of NOTCH1 in the isoform-specific merlin knockout nerve lysates (Fig. 1B) might be caused by merlin deficiency in Schwann cells.

To further validate our observations, we conditionally deleted merlin in the neuronal cell compartment using a mouse line that expresses Cre recombinase under the neuron-specific promoter *Nefh* (Nefh-Cre;Nf2flox). The neuron-specific loss of merlin (Nefh-Cre;Nf2$^{fl/fl}$) resulted in a considerable reduction of NRG1 type III in sciatic nerve lysates when compared with wild-type control mice (Nefh-Cre;Nf2$^{+/+}$). This reduction in NRG1 type III was again accompanied by a simultaneous decrease of Akt phosphorylation (Fig. 1E). Most strikingly, a comparable decline in NRG1 type III expression also occurred in mice bearing heterozygous loss of merlin in neurons (Nefh-Cre;Nf2$^{fl/+}$), indicating that

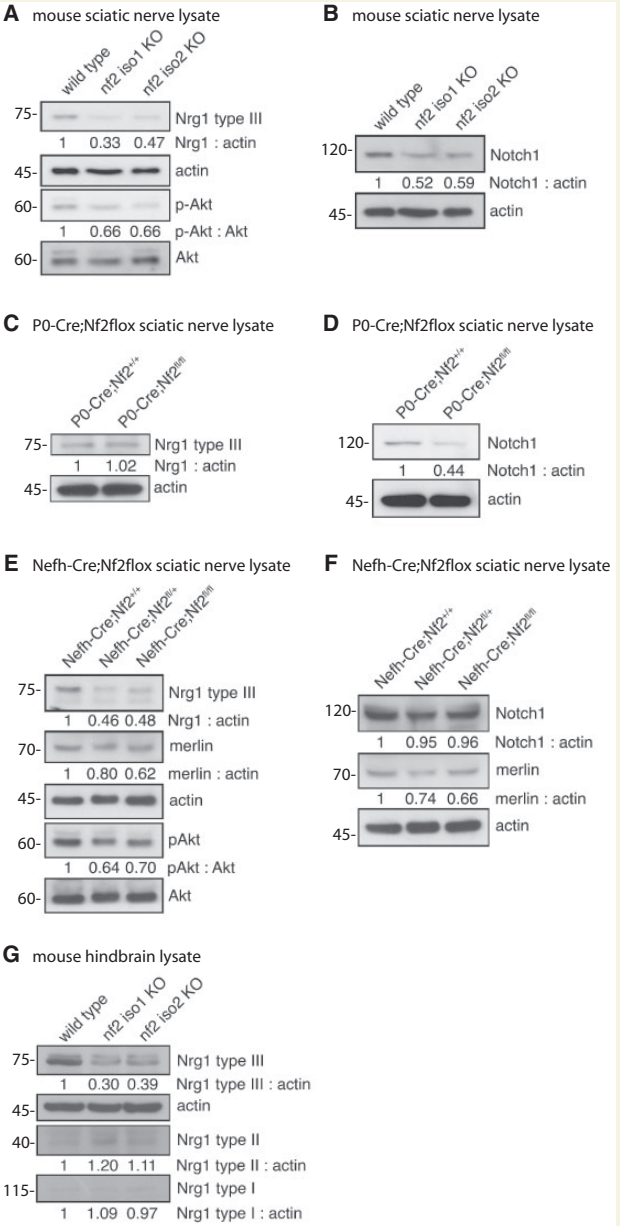

Figure 1 Loss of merlin in sciatic nerve lysates is accompanied by decreasing NRG1 type III levels. (**A–F**) Immunoblots of sciatic nerve lysates taken from adult mice. (**A**) Loss of each major merlin isoform in transgenic animals (nf2 iso1 KO; nf2 iso2 KO) results in decreased expression of NRG1 type III and reduced Akt phosphorylation (p-Akt). Actin was used as loading control ($n = 3$). (**B**) Loss of merlin-iso1 or merlin-iso2 *in vivo* leads to reduced expression of NOTCH1 ($n = 2$). (**C** and **D**) Schwann cell-specific loss of merlin (P0-Cre;Nf2$^{fl/fl}$) has no effect on NRG1 type III level but lowers NOTCH1 expression compared with wild-type littermates (P0-Cre;Nf2$^{+/+}$; $n = 3$). (**E** and **F**) Neuron-specific merlin knockout (Nefh-Cre;Nf2flox$^{fl/fl}$) reduces levels of NRG1 type III and p-Akt. NOTCH1 levels are unchanged in sciatic nerves after loss of merlin in the neuronal compartment ($n = 2$). (**G**) Isoform-specific loss of merlin reduces NRG1 type III amounts in hind-brain lysates of adult mice ($n = 3$). Blot quantifications (density values) are depicted below respective lanes and are normalized to actin and wild-type controls. KO = knockout.

reduction of merlin gene dosage to one allele is sufficient to alter NRG1 expression. Please note that the neuron-specific loss of merlin is reflected only by a slight reduction in the overall merlin protein level detected by western blot from sciatic nerve lysates (Fig. 1E and F). This in turn suggests that the majority of the merlin protein found in the lysates is of non-neuronal origin (Schwann cells, fibroblasts etc.).

To further underscore the functional importance of heterozygous merlin mutations *in vivo*, we studied mice bearing only one functional merlin allele in all cells of the body ($Nf2^{\Delta/fl}$ described above), a condition that mimics NF2 germline mutations where only one functional merlin allele remains. Loss of one functional merlin allele was again sufficient to detect reduced NRG1 type III levels ($Nf2^{\Delta/fl}$ in Supplementary Fig. 2). In contrast, the neuron-specific loss of merlin had no obvious effect on Notch1 expression in sciatic nerve lysates (Fig. 1F), confirming that the reduction of expression of Notch1 in complete isoform merlin knockout nerve lysates (Fig. 1B) is caused by reduced expression in Schwann cells.

In addition to lysates derived from PNS nerves, NRG1 type III expression was also reduced in hind-brain lysates of merlin-deficient adult mice (Fig. 1G), indicating that merlin's involvement in NRG1 expression applies to both PNS and CNS neurons. The expression of NRG1 types I and II, however, appeared mostly unchanged after the loss of merlin. In conclusion, these results indicate that the loss of both major merlin isoforms in the neuronal compartment affects the expression of the axonal surface protein NRG1 type III.

Hypermyelination in merlin knockout animals

According to the literature, the NRG1 type III axonal signal controls the fine-tuning of myelin membrane growth. We therefore expected that the observed reduction of NRG1 type III levels *in vivo* should result in hypomyelination (thinner myelin) during development (Michailov *et al.*, 2004). The g-ratio is a measure of myelin thickness and is proportional to fibre size (axon diameter/myelinated fibre diameter). We therefore analysed this typical myelination parameter in sciatic nerve cross-sections from both merlin-iso2- and merlin-iso1-deficient animals (Fig. 2A and Supplementary Fig. 3).

Surprisingly, visual inspection of myelinated axons of both merlin isoform-specific knockout animals did not show a drop in myelination. Instead, a slight but significant increase in myelin thickness could be observed (Fig. 2B, left panel). Consequently, the g-ratio was decreased in both mouse strains (Fig. 2B, right panel). The myelination of P0-Cre;Nf2flox mice, where merlin is specifically deleted in Schwann cells only, instead appeared decreased (Fig. 2C), resulting in a g-ratio gain because the axon diameter was also statistically reduced (not shown).

Collectively, our data indicate a specific reduction in NRG1 type III as well as a decrease in the signalling cascades downstream of the ERBB2/3 receptor with loss of merlin isoform 1 or 2. However, surprisingly we can detail the resulting Schwann cell phenotype is hypermyelination rather than hypomyelination.

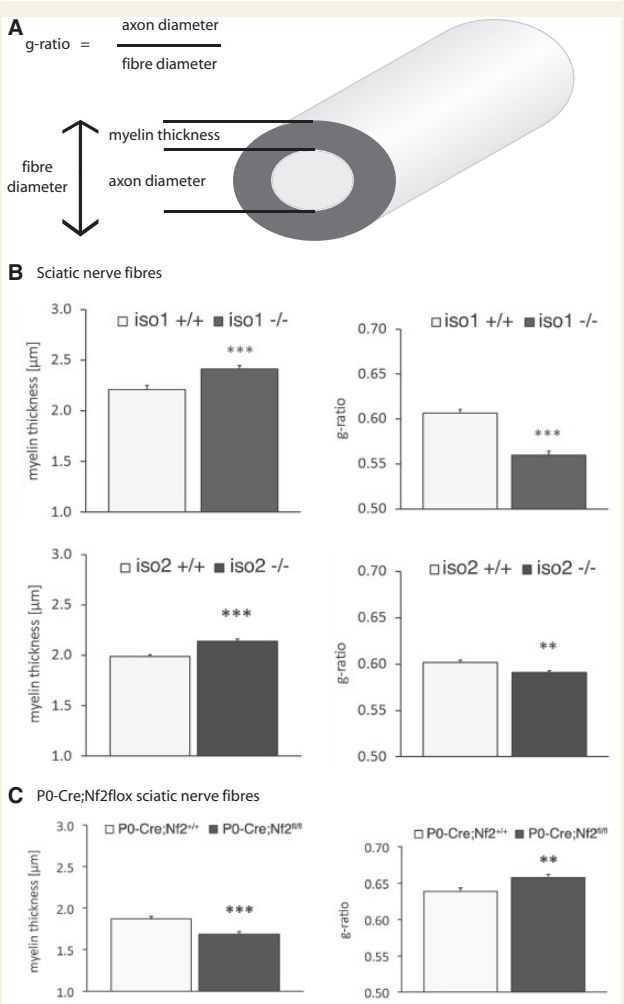

Figure 2 Merlin knockout animals show altered myelination. (**A**) Schematic diagram indicating important nerve fibre parameters. (**B** and **C**) Myelination thickness and g-ratio quantifications of sciatic nerves taken from (**B**) merlin isoform-specific knockout animals (iso1 -/-; iso2 -/-) and wild-type littermates (iso1 +/+; iso2 +/+) as well as from (**C**) P0-Cre;Nf2flox mice bearing a Schwann cell-specific merlin loss (data represent mean ± SEM; $^{**}P < 0.01$; $^{***}P < 0.001$; $n > 300$).

NRG1 expression following merlin overexpression *in vitro*

To further test whether merlin can affect the levels of NRG1 type III *in vitro*, we performed cell culture experiments with neuronally differentiated P19 cells (Jones-Villeneuve *et al.*, 1982) and primary dorsal root ganglion cells. Overexpression of either full length merlin-iso1 or merlin-iso2 in P19 cells resulted in elevated protein expression of NRG1 type III compared to vector control (Fig. 3A). Moreover, we transfected FLAG-tagged merlin fragments into P19 cells to identify the protein domain important to this effect. We found that the C-terminal fragments of both major merlin isoforms predominantly increased NRG1 type III expression in P19 cells whereas the N-terminus, which is shared by both major merlin isoforms, showed no significant effect (Fig. 3A). We additionally

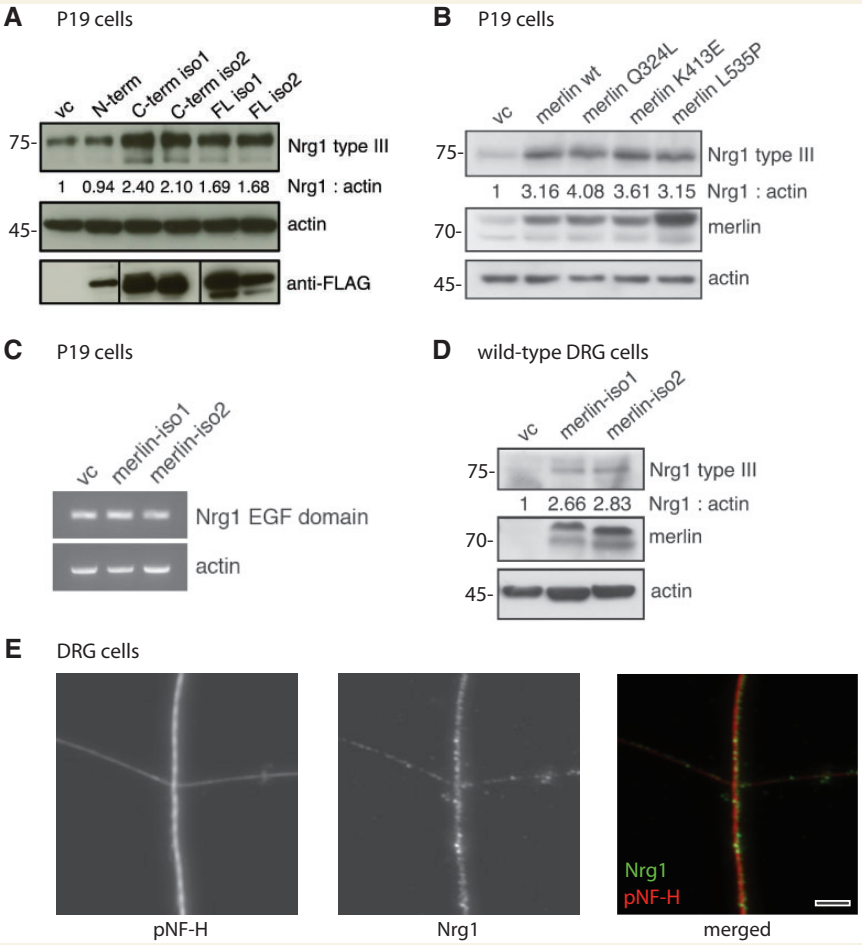

Figure 3 Merlin overexpression *in vitro* induces NRG1 type III expression. (**A**) Immunoblot of P19 cell lysates after transfection of different FLAG-tagged merlin fragments. Transfection of empty vector was used as control (vc); actin indicates equal loading. Anti-FLAG staining shows transfection rate of each construct ($n = 3$). (**B**) Wild-type merlin isoform 1 (merlin wt) and merlin constructs bearing indicated C-terminal point mutations were transfected into P19 cells. Immunoblot shows NRG1 type III levels as well as merlin and actin as transfection and loading control, respectively ($n = 2$). Blot quantifications (density values) are depicted below respective lanes and are normalized to actin and transfection controls (vc). (**C**) Reverse-transcription PCR of P19 cell lysates following overexpression of merlin-iso1 or merlin-iso2 constructs. EGF domain-specific primers were used to detect *Nrg1* transcripts. Actin was used as loading control ($n = 3$). (**D**) Immunoblot of lysates derived from primary dorsal root ganglion (DRG) cells after merlin overexpression *in vitro* ($n = 3$). Blot quantifications (density values) are depicted below respective lanes and are normalized to actin and transfection controls (vc). (**E**) Immunostaining of primary dorsal root ganglion cells shows localization of NRG1 (green) in axons of cultured dorsal root ganglions (4 days *in vitro*). Axons were stained for phosphorylated neurofilaments as an axonal marker (pNF-H, red). Scale bar = 5 μm. N-term = N-terminal fragment; C-Term = C-terminal fragment; FL = full length.

tested whether known C-terminal merlin missense mutations derived from patients with NF2 (Yang *et al.*, 2011) (Q324L, K413E and L535P) affected merlin's ability to increase NRG1 type III levels *in vitro*. However, these NF2-derived point mutations showed no alteration with respect to NRG1 type III expression when compared with wild-type merlin (Fig. 3B). Taken together, these results verify that merlin can indeed modulate NRG1 type III and that the C-terminus of both isoforms 1 and 2 are important for this regulation. In addition, we conclude that complete loss of merlin or large truncations of merlin because of nonsense or frameshift mutations might have a functional consequence.

As NRG1 protein expression can be regulated both at the transcriptional and translational level (Velanac *et al.*, 2012), we examined whether merlin overexpression in P19 cells induces transcriptional upregulation of *Nrg1* messenger RNA levels. Using *Nrg1*-specific primers amplifying a product within the EGF domain, shared by *Nrg1* types I, II and III (Kerber *et al.*, 2003), we found that *Nrg1* messenger RNA expression appeared unchanged following merlin overexpression (Fig. 3C). These findings indicate that merlin does not regulate *Nrg1* at the messenger RNA level, but rather possibly influences its protein stability and/or cleavage.

To further verify our finding we analysed the actions of merlin in primary dorsal root ganglion cells. Overexpression of one major merlin isoform in dorsal root ganglion cells consistently led to increased NRG1 type III levels (Fig. 3D). In addition, immunostaining of NRG1 with phosphorylated neurofilaments as an axonal

marker in cultured dorsal root ganglion cells showed an expression pattern clearly resembling an axonal surface molecule (Fig. 3E).

We next performed a morphometric analysis of NRG1 expression on nerve specimens of merlin-iso1 knockout mice as representative for merlin loss *in vivo* and corresponding wild-type littermates (Fig. 4A). Evaluation of the stainings revealed no significant difference in 3-week-old animals concerning the percentage of NRG1-positive myelinated fibres (Fig. 4B). However, in 8-week-old mice a significant decrease in the percentage of NRG1-positive fibres was found in merlin-iso1-deficient animals compared with wild-type controls (Fig. 4C). This indicates that sciatic nerve tissue of merlin knockout mice exhibits an age-dependent downregulation of NRG1 type III.

NRG1 expression in human sural nerve biopsies

To underline the clinical relevance of our findings, we analysed human sural nerve biopsies from seven patients with NF2, healthy control individuals, and reference samples showing neuropathies of different aetiologies. The age and gender of the investigated patients with NF2 did not differ significantly from those of the control group (mean age NF2: 44 ± 11.63 years, controls: 55 ± 11.96 years). The percentage of NRG1-positive myelinated fibres as indicated by expression of myelin protein zero was significantly lower in NF2 samples compared with controls and with chronic inflammatory demyelinating polyneuropathy and axonopathy samples (mean value for NF2: $20\% \pm 13\%$, for controls: $77\% \pm 16\%$, for chronic inflammatory demyelinating polyneuropathy: $61\% \pm 12\%$ and for axonopathy: $45\% \pm 13\%$; NF2 versus controls: $P < 0.001$, NF2 versus chronic inflammatory demyelinating polyneuropathy: $P < 0.001$, NF2 versus axonopathy: $P = 0.004$). In addition, chronic inflammatory demyelinating polyneuropathy and axonopathy samples showed significantly reduced percentages of NRG1-positive myelinated fibres when compared with controls ($P = 0.014$ for controls versus chronic inflammatory demyelinating polyneuropathy, $P < 0.001$ for controls versus axonopathy). Comparing all four groups, the reduction of NRG1-positive fibres was most prominent in patients with NF2 (Fig. 5A and B). Besides, fibre density quantifications of the same samples revealed that biopsies taken from patients with NF2 show the lowest number of axons per mm^2 indicating a severe chronic axonopathy (Fig. 5C). To verify the histomorphological results in terms of NRG1 levels, we also conducted immunoblotting to determine the expression of NRG1 type III in sural nerve biopsies of patients with NF2 and healthy control ssubjects. Consistently, lysates of

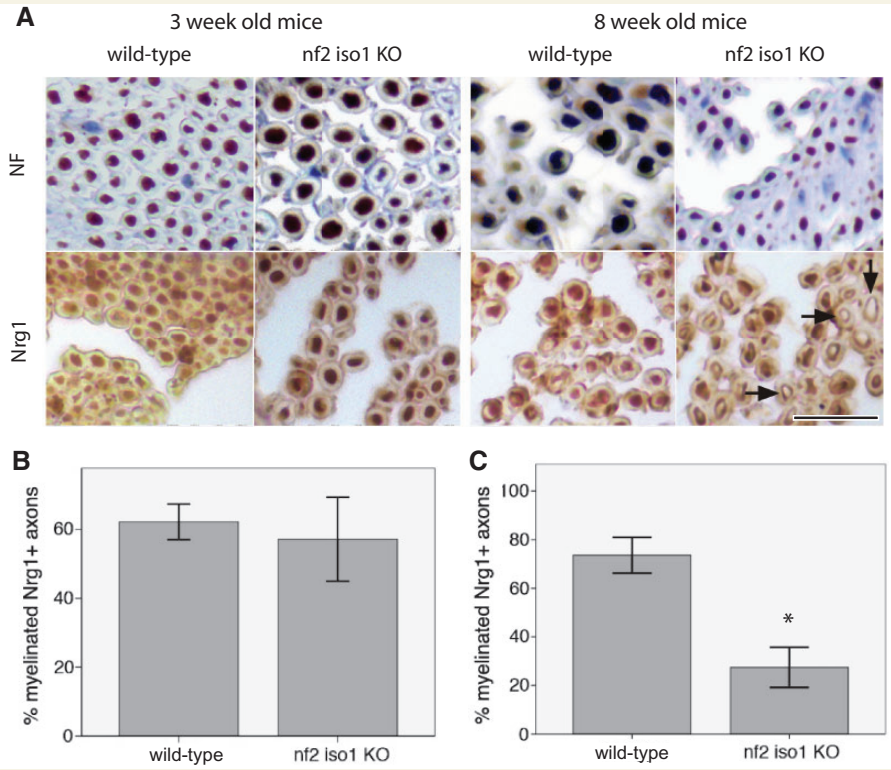

Figure 4 Sciatic nerve axons of merlin knockout mice show reduced axonal NRG1 expression. (**A**) Representative pictures of immunohistochemical stainings for neurofilaments (NF) and NRG1 on sciatic nerves of merlin isoform1-deficient mice (nf2 iso1 KO) and wild-type controls. Visualization of bound antibodies with diaminobenzidine (brown), counterstained with Mayer's haemalum. Scale bar = 20 μm. Arrows indicate examples of unstained axons. (**B** and **C**) Percentage of NRG1-positive myelinated fibres in sciatic nerve samples of 3-week-old (**B**) and 8-week-old (**C**) nf2 iso1 knockout (KO) mice and corresponding wild-type littermates (data represent mean ± SEM; $^*P < 0.05$).

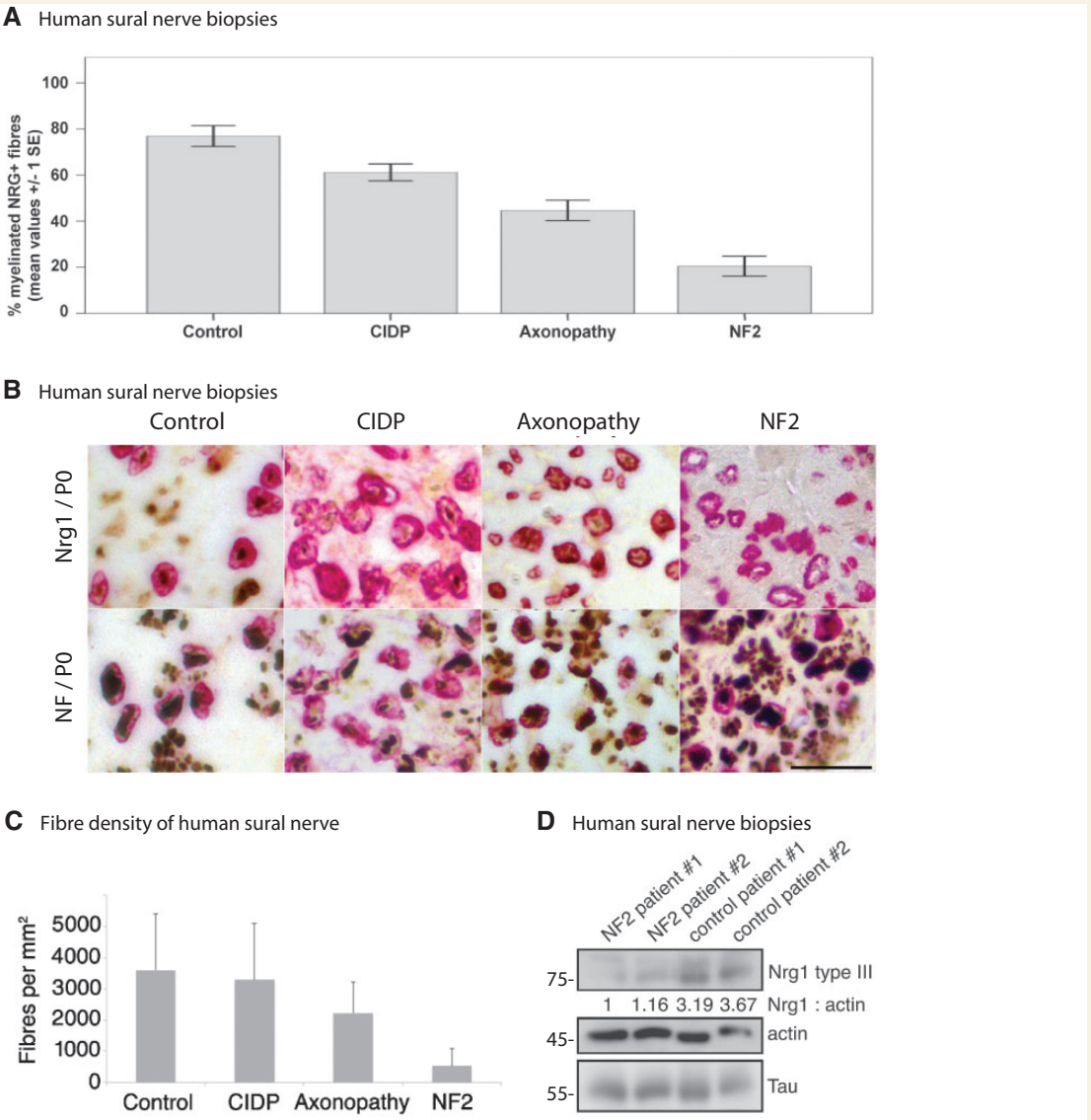

Figure 5 Sural nerve biopsies of NF2 patients show reduced NRG1 type III levels. (**A**) Percentage of NRG1-positive myelinated fibres in nerve samples of healthy control individuals versus chronic inflammatory demyelinating polyneuropathy (CIDP), axonopathy and patients with NF2 (data represent mean ± SEM; for significance levels see 'Results' section). (**B**) Expression of NRG1/myelin protein zero (P0) versus neurofilament (NF)/myelin protein zero in sural nerve biopsies of healthy control individuals as well as chronic inflammatory demyelinating polyneuropathy, axonopathy and patients with NF2. Typical examples of immunohistochemical double-labelling. Visualization of bound neurofilament (NF) and NRG1 antibodies with diaminobenzidine (brown) and of myelin protein zero antibodies with fast red (red), counterstained with Mayer's haemalum. Scale bar = 20 μm. (**C**) Sural nerve fibre densities per mm^2 of indicated disease conditions (data represent mean ± SEM). (**D**) Sural nerve biopsies of patients with NF2 and healthy control subjects were lysed and immunoblotted for NRG1 type III. Actin and the axonal marker tau served as loading control ($n = 3$). Blot quantifications (density values) are depicted below respective lanes and are normalized to actin and healthy control samples.

sural nerves from two patients showed significantly reduced NRG1 type III protein levels as compared to two control specimens (Fig. 5D).

ERBB2 receptor upregulation following neuronal loss of merlin

Upon loss of neuronal merlin a reduction in NRG1 type III levels was detected. Surprisingly we observed a hypermyelination of nerve fibres in these merlin-deficient animals *in vivo*. We therefore speculated that the ERBB2 receptor expression on Schwann cells might be increased in compensation to the reduced levels of NRG1 type III. We first performed morphometric analysis of ERBB2 receptor expression on nerve specimens of merlin-iso1 knockout mice and corresponding wild-type littermates (Fig. 6A). The number of ERBB2-positive myelinated fibres appeared significantly upregulated in 8-week-old knockout mice (Fig. 6B). Consistently, sciatic nerve lysates of mice lacking merlin in an isoform-specific manner also show elevated levels of ERBB2 detected by western blotting (Fig. 6C).

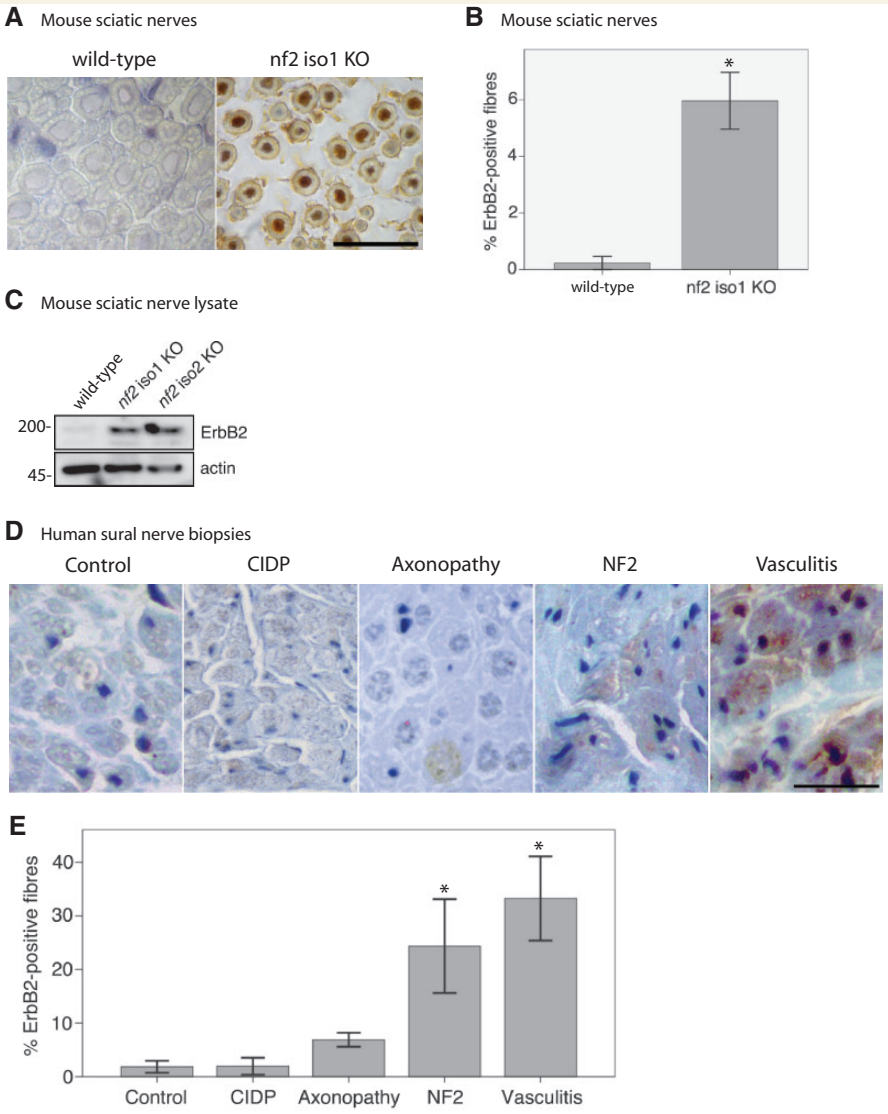

Figure 6 ERBB2 expression is upregulated in sural nerve biopsies of patients with NF2. (**A**) Representative examples of immunohistochemical stainings for ERBB2 on mouse sciatic nerves deficient of merlin isoform 1 (nf2 iso1 KO) and wild-type controls. Visualization of bound antibodies with diaminobenzidine (brown), counterstained with Mayer's haemalum. Scale bar = 20 μm. (**B**) Related quantifications to (**A**) of ERBB2-positive fibres in wild-type mice and merlin isoform1 knockout animals (data represent mean ± SEM; $*P < 0.05$; $n = 3$). (**C**) Immunoblot of sciatic nerve lysates showing that the loss of both major merlin isoforms *in vivo* is accompanied by increased ERBB2 levels ($n = 2$). Blot quantifications (density values) are depicted below respective lanes and are normalized to actin and wild-type samples. (**D**) Representative examples of immunohistochemical labelling of human sural nerve biopsies for ERBB2. Visualization of bound antibodies with diaminobenzidine (brown), counterstained with Mayer's haemalum. Scale bar = 20 μm. (**E**) Quantifications of ERBB2-positive fibres in biopsies of controls as well as patients suffering from chronic inflammatory demyelinating polyneuropathy (CIDP), axonopathy, NF2 and vasculitis (data represent mean ± SEM; $*P < 0.05$; $n = 3$).

In addition, we analysed human sural nerve biopsies of patients with NF2, healthy control individuals, and reference samples showing neuropathies of various aetiologies. Immunohistochemically, no ERBB2 labelling was detected in normal nerve tissue (Fig. 6D), but ERBB2 appeared markedly increased in pathological conditions with highest levels occurring in vasculitis followed by NF2, axonopathy and chronic inflammatory demyelinating polyneuropathy (Fig. 6E). Strikingly, upregulation of ERBB2 correlated with the decrease in NRG1-positive myelinated fibres ($P = 0.003$).

To verify our results and to exclude Schwann cell-intrinsic signalling events, we tested peripheral nerve tissue from mice bearing neuron-specific loss of merlin (Nefh-Cre;Nf2flox) for ERBB2 levels. Intriguingly, ERBB2 receptor expression was found to be upregulated following neuron-specific loss of merlin, whereas NRG1 levels appeared consistently lower (Fig. 7A and B). By immunoblotting we further found that merlin downregulation in neurons in both heterozygous and homozygous conditional merlin knockout mice, is associated with increased ERBB2 expression (Fig. 7C).

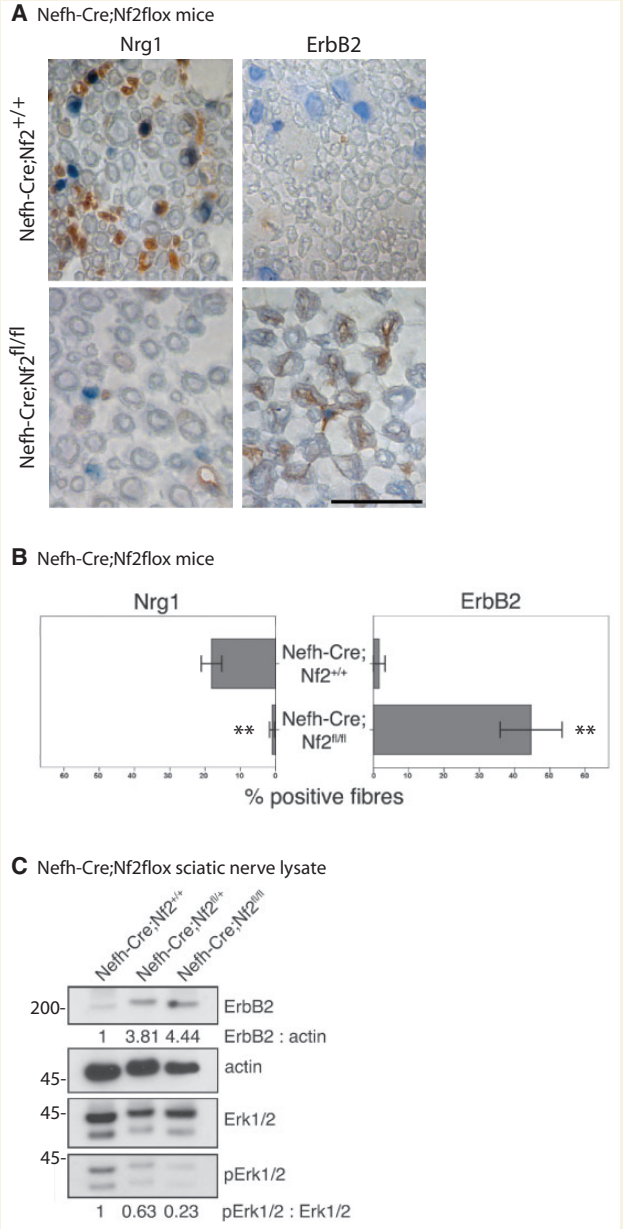

Figure 7 Neuron-specific loss of merlin is sufficient to increase ErbB2 levels on Schwann cells. (**A**) Representative pictures of immunohistochemical staining of mouse sciatic nerves taken from neuron-specific merlin knockout animals (Nefh-Cre;$Nf2^{fl/fl}$) and wild-type littermates (Nefh-Cre;$Nf2^{+/+}$). Visualization of antibodies raised against NRG1 and ERBB2 with diaminobenzidine (brown), counterstained with Mayer's haemalum. Scale bar = 20 μm. (**B**) Quantifications of NRG1 and ERBB2-positively labelled fibres in neuron-specific merlin knockout mice (Nefh-Cre;$Nf2^{fl/fl}$) and controls (data represent mean ± SEM, $^{**}P < 0.01$; $n = 3$). (**C**) Immunoblot of sciatic nerve lysates derived from homozygous (Nefh-Cre;$Nf2^{fl/fl}$) and heterozygous neuron-specific merlin knockout mice (Nefh-Cre;$Nf2^{fl/+}$) indicates elevated ERBB2 protein levels and decreased phosphorylation of Erk (pErk) compared with wild-type littermates (Nefh-Cre;$Nf2^{+/+}$; $n = 3$).

This indicates that increased ERBB2 levels in Schwann cells are a clear consequence of merlin loss in the neuronal compartment.

However, despite ERBB2 upregulation, sciatic nerve lysates of neuron-specific merlin knockout mice showed a reduced activation of the downstream signals indicated by reduced phosphorylation of Akt (Fig. 1A and E) as well as a member of the MAP kinase pathway Erk1/2 (Fig. 7C). Together our findings show that at least the two best known downstream target cues of ERBB2/3 receptors—PI-3K/Akt and MAP kinase pathway (Mei and Xiong, 2008)—show reduced activity despite increased ERBB2 levels. By immunohistochemistry on sciatic nerve cross-sections we could qualitatively show the primary source of Akt and Erk signalling to be of Schwann cell rather than axonal origin (Supplementary Figs 4 and 5).

Discussion

We report here a novel and clinically relevant finding concerning the tumour suppressor protein merlin, mutations of which are the cause of the hereditary tumour syndrome NF2. In addition to its well-established, growth-restricting functions in Schwann cells, we identified that axonally expressed merlin modifies Schwann cell activity. Taken together, we link merlin to one of the best-characterized signalling pathways of crosstalk between Schwann cells and axons, the NRG1–ERBB2/3 pathway. Our findings are of great importance because a highly interdependent relationship between Schwann cells and axons is required to maintain proper integrity and functionality of peripheral nerves throughout lifetime. In line with this notion, damage to one cell type invariably leads to pathophysiological changes in the other (Fricker and Bennett, 2011).

First of all, through regulation of decisive axonal surface proteins—namely NRG1 type III—the *Nf2* gene product determines the expression of growth factor-like molecules on axons important for Schwann cell actions such as proliferation and myelination. By means of different mouse models as well as sural nerve biopsies of patients with NF2, we could show that the loss of merlin or even reduction of merlin gene dosage in the neuronal compartment results in the downregulation of NRG1 type III. In contrast, loss of merlin specifically in Schwann cells had no effect on NRG1 type III expression.

How the loss of merlin in neurons mechanistically leads to a decrease in NRG1 type III levels is presently not clear. Our *in vitro* experiments showed that merlin overexpression in primary dorsal root ganglion cells and a neuronal cell line results in an increased level of the active NRG1 type III; a finding apparently independent of *Nrg1* gene expression regulation. Several studies have already identified a post-transcriptional regulation of neuregulins by different proteases such as BACE1 (Velanac *et al.*, 2012) or TACE (La Marca *et al.*, 2011) mediating cleavage and processing of NRG1 type III to its active form. Whether merlin modifies NRG1 type III levels through fine-tuning the activity of proteases remains to be established.

Several findings have suggested that reduced expression of axonal NRG1 type III in the PNS results in thinner myelination (Michailov *et al.*, 2004). It is therefore obscure why the *in vivo*

reduction of neuronal merlin, which is accompanied by reduced NRG1 type III levels, results in increased myelination. Intriguingly we detected an increase in ERBB2 receptor in Schwann cells, a likely compensatory reaction towards the reduced axonal expression of the ligand—NRG1 type III. This increase in ERBB2 receptor that functions as a co-receptor with EGFR, ERBB3 and ERBB4 could theoretically induce aberrant promyelination signals leading to the observed hyper-myelination.

However, when we traced the typical signalling activity downstream of ERBB2 in Schwann cells, such as phosphorylation of Akt or Erk, we found that these signals were rather decreased. It is plausible that an increase of ERBB2 may lead to other distinct downstream promyelinating signalling activities, for example the small GTPase RAC1. Moreover it is possible that there might exist other neuronal factors affected by merlin independent of the neuregulin network that determine myelination. For instance laminin/integrin (McKee *et al.*, 2012) and GPR126 (Monk *et al.*, 2011) signalling in Schwann cell myelination have already been shown. These extracellular cues may function independently and/or cooperatively with NRG1/ERBB2 signalling cascade to control myelination. These potentially key extracellular signalling alterations have not yet been tested in our system. Nonetheless it is clear that changes in merlin activity, specifically in the axon, modifies Schwann cell behaviour in part through an abnormal NRG1 type III–ERBB2 network leaving the peripheral nerve possibly vulnerable to abnormal maintenance and repair.

Interestingly, increased ERBB2 expression appears to be very specific to the loss of merlin in NF2 disease because sural nerve biopsy samples of patients with chronic inflammatory demyelinating polyneuropathy and axonopathy with decreased NRG1 type III levels did not show an upregulation of ERBB2 expression. Again, whether merlin regulates axonal factors in addition to NRG1 type III influencing ERBB2 expression on Schwann cells remains to be elucidated.

However, it is clear that particularly the loss of axonal merlin increases Schwann cell susceptibility towards mitogenic factors indicated by elevated ERBB2 levels. Merlin-deficient Schwann cells and human NF2 schwannomas have been previously shown to overexpress ERBB2 and ERBB3 receptor molecules (Lallemand *et al.*, 2009). Consequently, the ERBB2/3 receptor has been identified as a potential target for NF2 therapy (Clark *et al.*, 2008). The use of trastuzumab, a monoclonal antibody interfering with ERBB2 receptor activity, is already in clinical use in breast cancer therapy.

Taken together, our data indicate that ERBB2/3 expression levels in Schwann cells are controlled by both merlin levels within Schwann cell themselves (Lallemand *et al.*, 2009) as well as by the axonal compartment through the NRG1 type III signalling, as identified here.

Further functional studies are required to elucidate a possible contribution of axonal merlin to the early events of NF2-related tumour development. Presently, existing NF2 mouse models primarily focus on merlin loss in Schwann cells. Neuronal merlin, which is also affected by *Nf2* germline mutations, is not taken into account. New mouse models of the disease addressing the importance of the microenvironment of peripheral nerves are therefore required.

Acknowledgements

The authors would like to thank Heidi Rosemann, Sara Holly, Frank Kaufmann and Dominique Galendo for their skilled breeding and husbandry of animals. Stefanie Ramrath is acknowledged for her excellent technical assistance.

Funding

This work was supported by SFB 604, DFG MO 1421/2-1 and Krebshilfe 107089. A.S. is a recipient of a Young Investigator Award from the Children's Tumor Foundation (New York, USA).

Supplementary material

Supplementary material is available at *Brain* online.

References

Baser MER, Evans DG, Gutmann DH. Neurofibromatosis 2. Curr Opin Neurol 2003; 16: 27–33.

Clark JJ, Provenzano M, Diggelmann HR, Xu N, Hansen SS, Hansen MR. The ErbB inhibitors trastuzumab and erlotinib inhibit growth of vestibular schwannoma xenografts in nude mice: a preliminary study. Otol Neurotol 2008; 29: 846–53.

Corfas G, Velardez MO, Ko CP, Ratner N, Peles E. Mechanisms and roles of axon-Schwann cell interactions. J Neurosci 2004; 24: 9250–60.

El Bejjani R, Hammarlund M. Notch signaling inhibits axon regeneration. Neuron 2012; 73: 268–78.

Fricker FR, Bennett DL. The role of neuregulin-1 in the response to nerve injury. Future Neurol 2011; 6: 809–22.

Gutmann DH, Aylsworth A, Carey JC, Korf B, Marks J, Pyeritz RE, et al. The diagnostic evaluation and multidisciplinary management of neurofibromatosis 1 and neurofibromatosis 2. JAMA 1997; 278: 51–7.

Hagel C, Lindenau M, Lamszus K, Kluwe L, Stavrou D, Mautner VF. Polyneuropathy in neurofibromatosis 2: clinical findings, molecular genetics and neuropathological alterations in sural nerve biopsy specimens. Acta Neuropathol 2002; 104: 179–87.

Jones-Villeneuve EM, McBurney MW, Rogers KA, Kalnins VI. Retinoic acid induces embryonal carcinoma cells to differentiate into neurons and glial cells. J Cell Biol 1982; 94: 253–62.

Kerber G, Streif R, Schwaiger FW, Kreutzberg GW, Hager G. Neuregulin-1 isoforms are differentially expressed in the intact and regenerating adult rat nervous system. J Mol Neurosci 2003; 21: 149–65.

La Marca R, Cerri F, Horiuchi K, Bachi A, Feltri ML, Wrabetz L, et al. TACE (ADAM17) inhibits Schwann cell myelination. Nat Neurosci 2011; 14: 857–65.

Lallemand D, Manent J, Couvelard A, Watilliaux A, Siena M, Chareyre F, et al. Merlin regulates transmembrane receptor accumulation and signaling at the plasma membrane in primary mouse Schwann cells and in human schwannomas. Oncogene 2009; 28: 854–65.

Liu X, Bates R, Yin DM, Shen C, Wang F, Su N, et al. Specific regulation of NRG1 isoform expression by neuronal activity. J Neurosci 2011; 31: 8491–501.

Maguire HC Jr, Greene MI. Neu (c-erbB-2), a tumor marker in carcinoma of the female breast. Pathobiology 1990; 58: 297–303.

Malin SA, Davis BM, Molliver DC. Production of dissociated sensory neuron cultures and considerations for their use in studying neuronal function and plasticity. Nat Protoc 2007; 2: 152–60.

Massa R, Palumbo C, Cavallaro T, Panico MB, Bei R, Terracciano C, et al. Overexpression of ErbB2 and ErbB3 receptors in Schwann cells of

patients with Charcot-Marie-tooth disease type 1A. Muscle Nerve 2006; 33: 342–9.

Mckee KK, Yang DH, Patel R, Chen ZL, Strickland S, Takagi J, et al. Schwann cell myelination requires integration of laminin activities. J Cell Sci 2012; 125: 4609–19.

Mei L, Xiong WC. Neuregulin 1 in neural development, synaptic plasticity and schizophrenia. Nat Rev Neurosci 2008; 9: 437–52.

Michailov GV, Sereda MW, Brinkmann BG, Fischer TM, Haug B, Birchmeier C, et al. Axonal neuregulin-1 regulates myelin sheath thickness. Science 2004; 304: 700–3.

Miller SJ, Li H, Rizvi TA, Huang Y, Johansson G, Bowersock J, et al. Brain lipid binding protein in axon-Schwann cell interactions and peripheral nerve tumorigenesis. Mol Cell Biol 2003; 23: 2213–24.

Monk KR, Oshima K, Jors S, Heller S, Talbot WS. Gpr126 is essential for peripheral nerve development and myelination in mammals. Development 2011; 138: 2673–80.

Morrison H, Sherman LS, Legg J, Banine F, Isacke C, Haipek CA, et al. The NF2 tumor suppressor gene product, merlin, mediates contact inhibition of growth through interactions with CD44. Genes Dev 2001; 15: 968–80.

Morrissey TK, Levi AD, Nuijens A, Sliwkowski MX, Bunge RP. Axon-induced mitogenesis of human Schwann cells involves heregulin and p185erbB2. Proc Natl Acad Sci USA 1995; 92: 1431–5.

Nave KA, Salzer JL. Axonal regulation of myelination by neuregulin 1. Curr Opin Neurobiol 2006; 16: 492–500.

Quintes S, Goebbels S, Saher G, Schwab MH, Nave KA. Neuron-glia signaling and the protection of axon function by Schwann cells. J Peripher Nerv Syst 2010; 15: 10–6.

Rahmatullah M, Schroering A, Rothblum K, Stahl RC, Urban B, Carey DJ. Synergistic regulation of Schwann cell proliferation by heregulin and forskolin. Mol Cell Biol 1998; 18: 6245–52.

Schulz A, Baader SL, Niwa-Kawakita M, Jung MJ, Bauer R, Garcia C, et al. Merlin isoform 2 in neurofibromatosis type 2-associated polyneuropathy. Nat Neurosci 2013; 16: 426–33.

Schulz A, Geissler KJ, Kumar S, Leichsenring G, Morrison H, Baader SL. Merlin inhibits neurite outgrowth in the CNS. J Neurosci 2010; 30: 10177–86.

Taveggia C, Zanazzi G, Petrylak A, Yano H, Rosenbluth J, Einheber S, et al. Neuregulin-1 type III determines the ensheathment fate of axons. Neuron 2005; 47: 681–94.

Vartanian T, Goodearl A, Viehover A, Fischbach G. Axonal neuregulin signals cells of the oligodendrocyte lineage through activation of HER4 and Schwann cells through HER2 and HER3. J Cell Biol 1997; 137: 211–20.

Vavlitou N, Sargiannidou I, Markoullis K, Kyriacou K, Scherer SS, Kleopa KA. Axonal pathology precedes demyelination in a mouse model of X-linked demyelinating/type I Charcot-Marie Tooth neuropathy. J Neuropathol Exp Neurol 2010; 69: 945–58.

Velanac V, Unterbarnscheidt T, Hinrichs W, Gummert MN, Fischer TM, Rossner MJ, et al. Bace1 processing of NRG1 type III produces a myelin-inducing signal but is not essential for the stimulation of myelination. Glia 2012; 60: 203–17.

Yang C, Asthagiri AR, Iyer RR, Lu J, Xu DS, Ksendzovsky A, et al. Missense mutations in the NF2 gene result in the quantitative loss of merlin protein and minimally affect protein intrinsic function. Proc Natl Acad Sci USA 2011; 108: 4980–5.

Yoon K, Gaiano N. Notch signaling in the mammalian central nervous system: insights from mouse mutants. Nat Neurosci 2005; 8: 709–15.

Zhang HX, Li WQ, Zhang HS, Zhang Y, Zhao JP, Lv LX, et al. Expressional changes of neuregulin-1 gene mRNA in peripheral blood from schizophrenia patients. Zhonghua Yi Xue Yi Chuan Xue Za Zhi 2011; 28: 620–4.